

Atf İçin: Baran, A. ve Ertaş, E. (2025). Morin hidrat yüklü HPAC@MNP nanokompozitinin hazırlanması, karakterizasyonu ve in vitro uygulamaları. *İğdır Üniversitesi Fen Bilimleri Enstitüsü Dergisi*, 15(1), 217-227.

To Cite: Baran, A. & Ertaş, E. (2025). Preparation, characterization and in vitro applications of morin hydrate loaded HPAC@MNP nanocomposite. *Journal of the Institute of Science and Technology*, 15(1), 217-227.

Morin hidrat yüklü HPAC@MNP nanokompozitinin hazırlanması, karakterizasyonu ve in vitro uygulamaları

Ayşe BARAN^{1*}, Erdal ERTAŞ²

Öne Çıkanlar:

- Kanser hücresi
- Manyetik ilaç salınımı
- Morin Hidrat

Anahtar Kelimeler:

- FTIR
- HUVEC
- MCF-7
- U373
- Aktif karbon
- Nanopartikül

ÖZET:

Kanser, her yıl küresel olarak milyonlarca insanın hayatına mal olan, tüm yaş gruplarından ve etnik kökenlerden bireyleri etkileyen yaygın ve ölümcül bir hastalıktır. Kanser tedavisinde kullanılan ilaçlar ayırım gözetmeksizin hem kötü huylu hem de sağlıklı hücreleri etkilediği için, büyük olumsuz etkilere neden olmasının yanı sıra sistemik toksisiteye de neden olur. Son zamanlarda, ilaçların neden olduğu olumsuz etkileri en aza indirmek için belirli bölgeleri özel olarak hedef alan ilaç verme sistemleri geliştirildi. Morin (MRN), antiangiyojenik, antiinflamatuvar, antikanser ve antibakteriyel aktivitelerini araştırmak için yürütülen önemli araştırmaların konusu olan flavonol bazlı bir ilaçtır. Bu çalışma, alıç bitkisinden elde edilen biyoyumlu aktif karbon üzerine bir manyetik nanopartikül tabakası uygulanarak manyetik özelliklere sahip bir ürünün sentezini içermektedir. Alıç bitkisinden (HP) elde edilen aktif karbonun (AC) manyetik nanopartikülleri (MNP'ler) ile sentezlenen HPAC@MNP'lerin karakterizasyonu Fourier Transform Kızılötesi (FTIR), Taramalı Elektron Mikroskobu (SEM), Dinamik Işık Saçılımı (DLS) ve Zeta Potansiyeli ile karakterize edildi. DLS analizi, HPAC@MNP'lerin ve HPAC@MNPs-MRN'nin ortalama partikül boyutunun sırasıyla yaklaşık 105 nm ve 142 nm olduğunu hesaplandı. İlaç yüklü manyetik nanokompozit, MCF-7 (meme), U373 (Glioblastoma) kanser hücre hatları ve İnsan Göbek Kordonu Endotel Hücreleri (HUVEC) sağlıklı hücre hattı üzerindeki sitotoksik etkileri açısından değerlendirildi. HPAC@MNP'lerin MRN yükleme ve salım özellikleri analiz edildi. Sonuçlar, kapalı ilacın salım sırasında uzun bir yayılma süresi sergilediğini gösterdi. Özetle, HPAC@MNPs manyetik nanokompozit taşıyıcıların kullanımı, MRN ilaçlarını belirli bölgelere etkili bir şekilde ulaştırmak için büyük bir potansiyele sahip olabilir.

Preparation, characterization and in vitro applications of morin hydrate loaded HPAC@MNPs nanocomposite

Highlights:

- Cancer cell
- Magnetic drug release
- Morin Hydrate

Keywords:

- FTIR
- HUVEC
- MCF-7
- U373
- Activated carbon
- Nanoparticle

ABSTRACT:

Cancer is a prevalent and fatal illness that claims the lives of millions of people globally every year, impacting individuals across all age groups and ethnicities. Because drugs that are used to treat cancer affect both malignant and healthy cells without discrimination, they are responsible for systemic toxicity in addition to creating major adverse effects. Recently, drug delivery systems that specifically target specific sites have been developed to minimize adverse effects caused by drugs. Morin (MRN) is a flavonol-based drugs that has been the subject of substantial research that has been conducted to investigate its antiangiogenic, anti-inflammatory, anticancer, and antibacterial activities. This study included the synthesis of a product with magnetic properties by applying a layer of magnetic nanoparticles onto biocompatible activated carbon derived from the hawthorn plant. Characterization of HPAC@MNPs synthesized with magnetic nanoparticle (MNPs) of activated carbon (AC) obtained from hawthorn plant (HP) was confirmed by Fourier Transform Infrared (FTIR), Scanning Electron Microscope (SEM), dynamic light scattering (DLS) and Zeta Potential. DLS analysis calculated the average particle size of HPAC@MNPs and HPAC@MNPs-MRN to be about 105 nm and 142 nm, respectively. The drug-loaded magnetic nanocomposite was evaluated for its cytotoxic effects on MCF-7 (breast), U373 (Glioblastoma) cancer cell lines, and Human Umbilical Vein Endothelial Cells (HUVEC) healthy cell line. The MRN loading and release characteristics of HPAC@MNPs were analyzed. The results indicated that the enclosed medication exhibited a prolonged spreading time during release. In summary, the use of HPAC@MNPs magnetic nanocomposite carriers may have great potential to effectively deliver MRN drugs to specific sites.

^{1*}Ayşe BARAN ([Orcid ID: 0000-0002-2317-0489](https://orcid.org/0000-0002-2317-0489)), Mardin Artuklu University, Graduate Education Institute, Department Of Biology, Mardin, Türkiye.

²Erdal ERTAŞ ([Orcid ID: 0000-0002-0325-1257](https://orcid.org/0000-0002-0325-1257)), Batman University, Department of Food Technology, Vocational School of Technical Sciences, 72000 Batman, Turkey.

*Sorumlu Yazar/Corresponding Author: Ayşe BARAN, e-mail: ayse.gorgec43@gmail.com

Bu çalışma daha önce bir yere gönderilmemiştir ve herhangi bir tezden üretilmemiştir.

INTRODUCTION

Cancer is an extremely challenging and life-threatening disease that results in a significant number of fatalities globally each year (Sleeman et al., 2021). Cancer presents a challenge in terms of treatment options and is often seen as a complex disease to manage, primarily due to delayed diagnosis and treatment (Barrios, 2022). Furthermore, the techniques employed for cancer treatment, such as surgical intervention, radiation, and chemotherapy, carry the risk of severe and sometimes fatal adverse reactions (Kamrani et al., 2023). Scientists and researchers are currently dedicated to creating methods that enable medications to specifically target a certain location of the human body. What determines whether a chemotherapy drug is effective is both the drug itself and the way the dose is administered to the diseased area. Iron oxide (Fe_3O_4) nanoparticles, also known as MNPs, have recently attracted a lot of attention due to the fact that they have the potential to be utilized in a wide range of biological applications (Aisida et al., 2020). Immunoassay, magnetic resonance imaging, bioseparators, and targeted medication administration through the use of an external magnetic field are some of the applications that fall under this category (Shabatina et al., 2020). Additionally, MNPs offer advantageous properties such as biocompatibility and low toxicity over other materials. They have an advantage over others thanks to that trait. Furthermore, magnetic nanoparticles can be easily produced by a range of techniques, such as micro-emulsion, ultra sound irradiation technology, and co-precipitation, to name just a few of the available options (Setia et al., 2023). MNPs core acts as a carrier for targeting, while the activated carbon (AC) coating derived from the HP (hawthorn plant was preferred because of the different photochemicals it contains in its structure and because it offers the opportunity to be used especially for biological samples) on MNPs offers functional groups and generates additional binding sites (Venskutonis, 2018). The HPAC has the ability to attach to magnetic nanoparticles (HPAC@MNPs) either through adsorption or covalent bonding. Additionally, it can interact with the anticancer medication morin hydrate (MRN) due to the presence of active functional groups in HPs structure.

MRN (3,5,7,2',4'-pentahydroxyflavone, Figure 1), is a member of the flavonoids groups that has been reported as an important agent effective various protective systemic effects, antioxidant, anti-inflammatory, antitumoral and antibacterial properties used for the treatment of cancer (Taguchi et al., 2020).

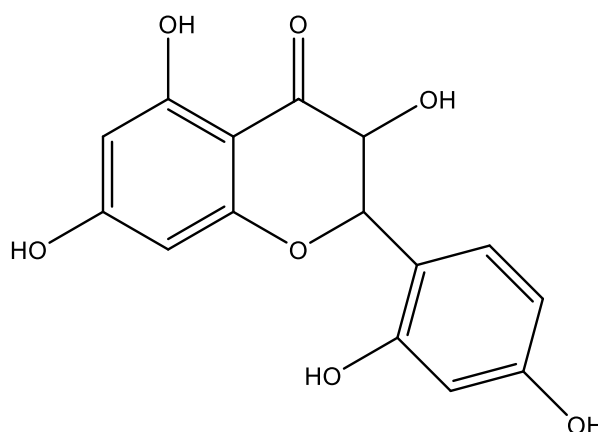


Figure 1. MRN chemical structure

The purpose of this research was to evolve a nanocomposite that possessed magnetic properties. This was accomplished by covering biocompatible activated carbon that was derived from the hawthorn plant with magnetic nanoparticles. The synthesized activated carbon-coated magnetic nanocomposite (HPAC@MNPs) was characterized using Fourier Transform Infrared (FTIR), Scanning Electron

Microscopy (SEM), dynamic light scattering (DLS), and Zeta Potential. The drug-loaded magnetic nanocomposite was tested for its cytotoxic effects on various cancer cell lines, including MCF-7 (breast) and U373 (Glioblastoma), as well as on the healthy cell line Human Umbilical Vein Endothelial Cells (HUVEC). A study was conducted to analyze the loading and release behavior of a nanocomposite consisting of activated carbon-coated magnetic nanoparticles. HPAC@MNPs magnetic nanocomposite carriers have the potential to demonstrate good results in terms of the delivery of MRN medication to the location that is intended for it.

MATERIALS AND METHODS

Chemicals and Reagents

Ferric chloride hexahydrate ($\text{FeCl}_3 \cdot 6\text{H}_2\text{O}$), ferrous sulfate heptahydrate ($\text{FeSO}_4 \cdot 7\text{H}_2\text{O}$), hydrochloric acid (HCl), sodium hydroxide (NaOH), ammonium hydroxide (NH_4OH), Morin hydrate, methanol, ethanol and zinc chloride (ZnCl_2) were purchased from Sigma-Aldrich (St. Louis, MO, USA). All other chemicals were of analytical grade and double distilled water was used in the experiments in the study.

In the study, leaves and fruits of the hawthorn (HP) plant collected from the Mardin Artuklu University campus area in September 2023 were used. This plant is called *Crataegus monogyna* in Latin.

An examination of the viability of the cells was conducted out at the Cell Culture Laboratory of the Dicle University Faculty of Veterinary Medicine Laboratory. The HUVEC cell line, which represents a healthy cell line, and the MCF-7 and U373 cell lines, which represent cancer cell lines, were acquired from the "American Type Culture Collection" (ATCC).

Characterization

Analysis of HPAC, HPAC@MNPs and HPAC@MNPs-MRN

The structural properties and morphology of the synthesized MRN, HPAC@MNPs, and HPAC@MNPs-MRN were characterized using the following methods:

Attenuated total reflectance-fourier transform infrared spectroscopy (ATR-FTIR); In order to determine the functional groups of MRN, HPAC@MNPs and HPAC@MNPs-MRN materials, Attenuated total reflectance-fourier transform infrared spectroscopy (ATR-FTIR) was performed with PerkinElmer Spectrum 100 instrument. ATR-FTIR spectra of MRN, HPAC@MNPs and HPAC@MNPs-MRN materials were obtained in the range of 4000 to 400 cm^{-1} . Spectrum outputs were measured with transmittance as a function of wave number.

Field Emission Scanning Electron Microscopy (SEM); HPAC@MNPs and HPAC@MNPs-MRN nanoparticles prepared for SEM analysis were imaged under a scanning electron microscope (ZEISS GEMINI 500) operated at 20 kV after being prepared by gold coating, and their surface morphologies were observed at different magnifications.

Zeta potential (ZP): Zeta potential analysis is an analysis method used to determine the surface charges of synthesized nanoparticles. In this analysis method, zeta potential measurement is important to understand the state of the nanoparticle surface and to estimate the long-term stability of the nanoparticle. In this study, the stability of HPAC@MNPs and HPAC@MNPs-MRN in solution was measured at 25 °C using Nano ZS90 from Malvern Instruments.

Dynamic light scattering (DLS); Dynamic light scattering technique is a most common optical measurement method to analyze the hydrodynamic particle size and the distribution of scattered light intensities over a range of dimensions defined by the Brownian motion of the particles in the submicron

range (5 nm–5 μ m). The size distributions of HPAC@MNPs and HPAC@MNPs-MRN were analyzed using the Malvern Mastersizer 2000 instrument.

Synthesis of HPAC

HP had multiple rinses with tap water. Subsequently, the plant was subjected to a thorough cleaning process involving agitation for 15 minutes at 200 rpm minute using distilled water. This procedure effectively eliminated any dust or dirt that had accumulated on the plant's surface. Following the cleaning procedure, the hawthorn plant was dried in the open air within at room temperature. Subsequently, the dried plant material was pulverized into a fine powder using an IKA M20 Universal grinder. The resulting powder was then kept in a container for future use in HPAC manufacture. 10 grams of the sample obtained by grinding the dried hawthorn plant was weighed and taken into a 1000 mL beaker. Then, 250 mL of a 25% zinc chloride solution was added and thoroughly mixed in a shaking water bath at a temperature of 80 °C for a duration of 60 minute. The resulting solid from the mixture, which was equilibrated to 25 °C and subsequently cooled, was transferred into a spacious container and subjected to desiccation in a 100 °C oven for a duration of 24 hours. Next, the dehydrated mixture was moved to porcelain crucibles and exposed to carbonization in a muffle furnace set at a temperature of 600 °C. The HPAC obtained after the carbonization process was left to cool in a desiccator at room temperature. To eliminate the residual zinc, chlorine, and other ions on the surface of HPAC, the surface was washed multiple times with a 0.01 M HCl solution. Following the treatment with hydrochloric acid (HCl), the HPAC was rinsed with deionized water until the pH reached a neutral level. Subsequently, it was dried using a lyophilizer (Santhosh and Dawn, 2021).

HPAC magnetic nanocomposite synthesis

The HPAC@MNPs magnetic nanocomposite was produced by applying a layer of HPAC, derived from the hawthorn plant, onto the surface of MNPs with certain adjustments, as documented in the literature (Peng ve ark. 2012). Following the dissolution of 6.0 grams of ferric chloride hexahydrate in one hundred milliliters of deionized water, a few drops (4-5) of 36.5% hydrochloric acid solution were introduced to the solution in order to hinder the oxidation of Fe^{3+} ions. The solution was then continuously mixed on a IKA C-mag HS 7 digital magnetic stirrer. The temperature of the mixture that had been obtained by adding 4.2 grams of iron sulfate heptahydrate to the solution that contained Fe^{3+} ions was raised to 90 °C. Following a time period of 30 minutes, a volume of 25 mL of concentrated ammonium hydroxide solution was gradually introduced to the mixture, leading to the formation of a solution with a black color. The resulting solution was continued to be stirred on the magnetic stirrer for another 30 min under the same conditions. Subsequently, a solution of 100 mg HPAC was introduced into the mixture by dissolving it in 150 mL of water. Following the addition of the solution containing HPAC, the product was agitated for an additional hour. After cooling to 25 °C, the resulting HPAC@MNPs magnetic nanocomposite was extracted from the solution medium using a neodymium magnet (Baran et al., 2024). The HPAC@MNPs magnetic nanocomposite underwent multiple washes with deionized water to eliminate any remaining contaminants from the reaction. Subsequently, the obtained product was dried at 40 °C using NÜVE EN 400 oven. After dried, the HPAC@MNPs magnetic nanocomposite was stored in a container of a distinct color for future use in research (Baran et al., 2024).

MRN drug loading studies

The MRN loading process involved distributing 50 mg of HPAC magnetic nanocomposite in a solution of 50 mL of methanol, which contained morin hydrate at a concentration of 100 μ g/mL. For the purpose of determining whether or not loading took place, a UV-VIS spectrophotometer was utilized. The incorporation of MRN into the HPAC@MNPs magnetic nanocomposite is accomplished by

agitating the solution at a speed of 200 revolutions per minute for a duration of 24 hours at ambient temperature. Then the particles were separated from the solution using an external magnet based on their magnetic properties. The concentration of MRN remaining in the solution was measured in a UV-Vis spectrometer at a wavelength of 385 nm. To calculate the drug loading, the MRN concentration in the supernatant was deducted from the starting MRN concentration. In the succeeding step, the HPAC@MNPs magnetic nanocomposite, which had been loaded with the drug, was isolated by means of a magnetic field, and then it was subjected to a drying process (Saif et al., 2015).

MRN drug release studies

For the purpose of the MRN release investigation, 10 mg of dry drug-loaded nanoparticles were subjected to analysis in solutions of pH 5.4 and 7.4 (the pH value of cancer cells is expressed as approximately 5-6. In this study, pH 5.4 was chosen as a value close to cancer cells. The pH 7.4 value was chosen because it is the natural pH) adjusted to 5 mL of Phosphate buffered saline (PBS) buffer. The solutions were stirred at 37 °C for 1, 3, 6, 12, 18, 24, 36, and 48 hours. After the specified incubation times, the samples were collected using a magnet and the amount of drug released was calculated using UV-vis spectrophotometry at 385 nm wavelength (Saif et al., 2015).

Cell Culture

An examination of the viability of the cells was conducted out at the Cell Culture Laboratory of the Dicle University Faculty of Veterinary Medicine Laboratory. The HUVEC cell line, which represents a healthy cell line, and the MCF-7 and U373 cell lines, which represent cancer cell lines, were acquired from the "American Type Culture Collection" (ATCC).

The chosen cell lines were cultured in a T75 flask using a cell culture media, as documented by Baran et al. (2023) the cells were then incubated at a temperature of 37 °C in an environment with 5% CO₂. Once the cells achieved 80-90% confluency, they were removed from the flasks and the number of cells was quantified using the hemocytometer method. The determined number of cells was added to 96-well plates three times, with 90 µl of medium added to each well, so that the cells would be 10x10⁵. Then, HPAC@MNPs-MRN solution at pH 7.4 and pH 5.4 was added to the microplates for two separate time applications of 24 and 48 hours. The cells were allowed to cling to the bottom of the microplate for a period of twenty-four hours. During the subsequent day, the seeded plates were treated with HPAC@MNPs-MRN pH 7.4 and HPAC@MNPs-MRN pH 5.4 at different concentrations, namely 1, 50, 100, and 200 µg/ml. The cells constituting the control group were treated with a liquid with pH 7.4 and 5.4 for HPAC@MNPs-MRN.

For the purpose of determining whether or not there were any changes in cell viability, in MTT test was carried out 24 and 48 hours after the treatment (Karimian et al., 2022). Afterward, 10 µl of the prepared MTT solution, which had a concentration of 5 mg/ml, was added to each well in the microplate that contained cells. The microplate was then incubated for three hours at 37 degrees Celsius in a humid atmosphere with 5% carbon dioxide. A total of one hundred microliters of dimethyl sulfoxide (DMSO) was added to each well after the medium had been withdrawn after a period of three hours. The optical density (OD) values of the wells were quantified using a UV/Vis Spectrophotometer following 20 minutes of agitation. The average absorbance values measured in the control wells were considered as the initial value for 100% live cell values. The absorbance values obtained from the HPAC@MNPs-MRN pH 7.4 and HPAC@MNPs-MRN in pH 5.4 applied wells were used to determine the percentage viability. This was done by comparing these values to the control absorbance value. The MTT trials were replicated thrice on distinct days.

Statistical analysis

In this study, in order to test the accuracy of the data, the experimental parameters were carried out in three repetitions on different days. In addition, the data were analyzed with the IBM SPSS 21.0 package program. In addition, Excel 2016 program was used to draw the graphics.

RESULTS AND DISCUSSION

FT-IR Analysis

Figure 2 presents the ATR-FTIR spectra of MRN, HPAC@MNPs, and HPAC@MNPs-MRN, along with the corresponding peaks representing each functional group. Upon analyzing the spectra of HPAC@MNPs and HPAC@MNPs-MRN, the presence of alkyne and C-H groups is indicated by the peaks observed at 2109 and 1990-1994 cm^{-1} , respectively. Furthermore, while examining the Figure 2, it is evident that the peaks observed at 1606 and 1695 cm^{-1} indicate the existence of the carbonyl ($-\text{C}=\text{O}$) stretching vibration group. Additionally, the peak at 1117 cm^{-1} signifies the presence of the (C-C-O) group resulting from the bonding of MRN (Cunha et al., 2023; Trendafilova et al., 2020). The signal seen at 537 cm^{-1} in the FTIR spectra of HPAC@MNPs and HPAC@MNPs-MRN, as shown in Figure 2, confirms the presence of a Fe-O bond. As seen in Figure 2, when the FTIR spectrum of the MRN drug is examined, the peaks seen at 3522 and 3082 cm^{-1} indicate the presence of hydroxyl groups. Moreover, the peak originating from the carbonyl group ($\text{C}=\text{O}$ stretching vibration) is at 1658 cm^{-1} . The $\text{C}=\text{C}$ stretching vibrations specific to the aromatic rings in the structure of MRN are seen at 1505 and 1453 cm^{-1} . The $\text{C}-\text{O}-\text{C}$ stretching vibrations (ether group) are located at 1304, 1226 and 1170 cm^{-1} (De Gaetano et al., 2023).

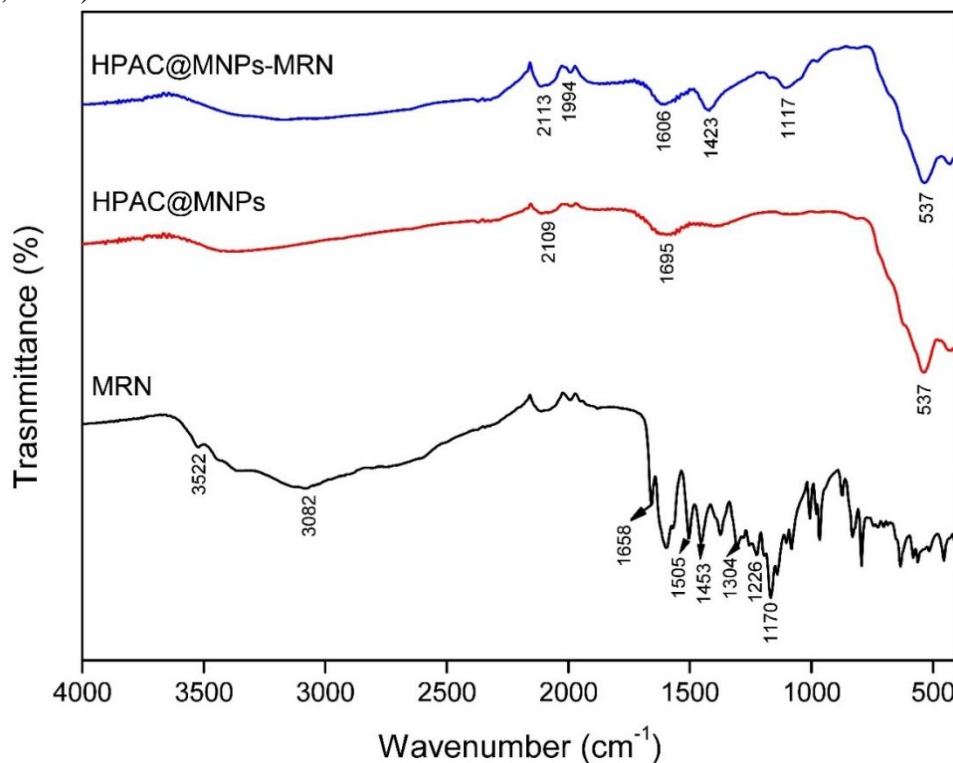


Figure 2. FTIR spectrum comparison MRN, HPAC@MNPs and HPAC@MNPs-MRN

SEM Analysis

The scanning electron microscope (SEM) was used for analyzing the surface images of HPAC@MNPs and HPAC@MNPs-MRN nanocomposites. In Figures 3a and 3b, SEM micrographs of these nanocomposites are displayed. A granular surface and a variety of pore sizes are characteristics of

the HPAC@MNPs nanocomposite. The irregular distribution of the drug in the surface morphology and porosity of HPAC@MNPs is the cause of the smoothness on the surface of the HPAC@MNPs nanocomposite that was obtained after the MRN drug was bound to the surface of the HPAC@MNPs nanocomposite. This smoothness was observed after the HPAC@MNPs-MRN nanocomposite was obtained (Baig et al., 2022; Tural et al., 2024).

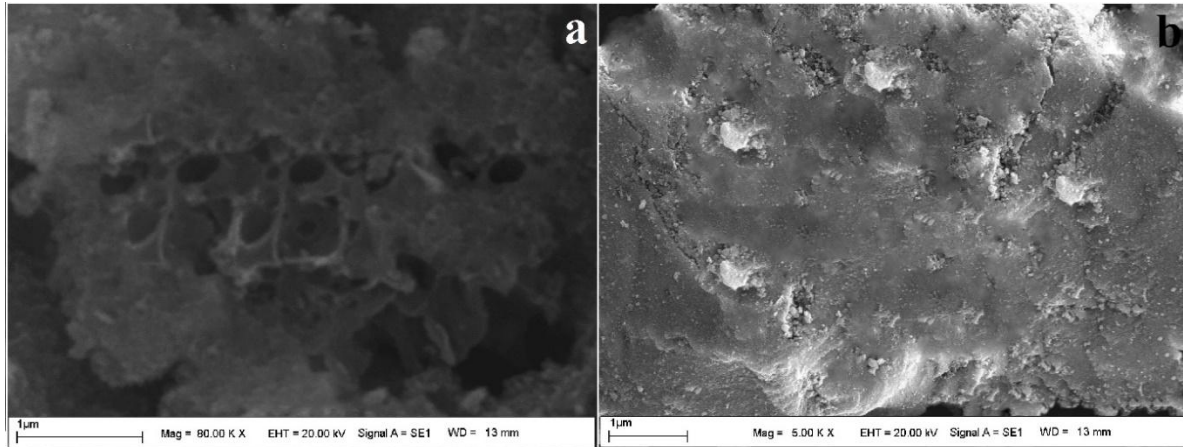


Figure 3. SEM images (a) HPAC@MNPs; (b) HPAC@MNPs-MRN

Particle size analysis

Figure 4 displays the findings of the DLS investigation on HPAC@MNPs and HPAC@MNPs-MRN nanocomposites. The analytical solution was generated by measuring the weight of 1 mg of HPAC@MNPs and HPAC@MNPs-MRN nanocomposites, and then subjecting them to sonication in 10 mL of deionized water using a probe sonicator. When evaluating the findings of the DLS analysis, it is shown that HPAC@MNPs and HPAC@MNPs-MRN nanocomposites had average size distributions of 105 nm and 142 nm, respectively (Kovrigina et al., 2022).

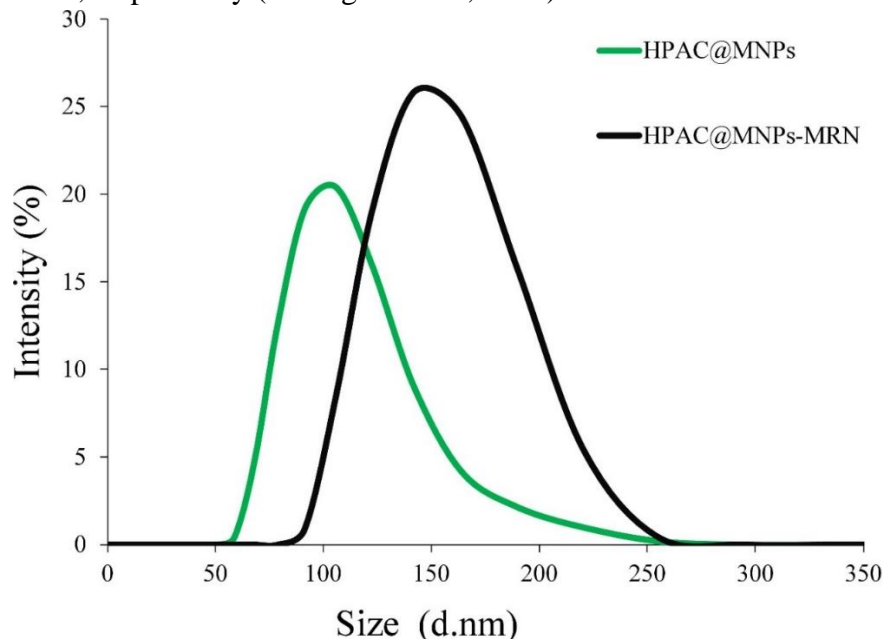


Figure 4. DLS analysis of HPAC@MNPs and HPAC@MNPs-MRN

Zeta potential analysis

Figure 5 displays the findings of the zeta potential examination performed on HPAC@MNPs and HPAC@MNPs-MRN for both of the products included in the study. Obtaining information about the

electric charge that is present on the surface of any substance can be accomplished by the measurement of the zeta potential. It is desirable to produce either high positive or low negative zeta potential values in order to avoid agglomeration of HPAC@MNPs and HPAC@MNPS-MRN and to ensure stability between these nanocomposites. If you want to achieve these goals, you should obtain either of these values. The measured potential values of HPAC@MNPs and HPAC@MNPS-MRN nanocomposites at the determined optimal circumstances were -16.8 and -17.2 mV, respectively. Upon examination of the data, it is evident that HPAC@MNPs and HPAC@MNPS-MRN exhibit minimal agglomeration as a result of their negatively charged nature. Consequently, the created suspensions retain their stability over an extended period (Attia et al., 2022).

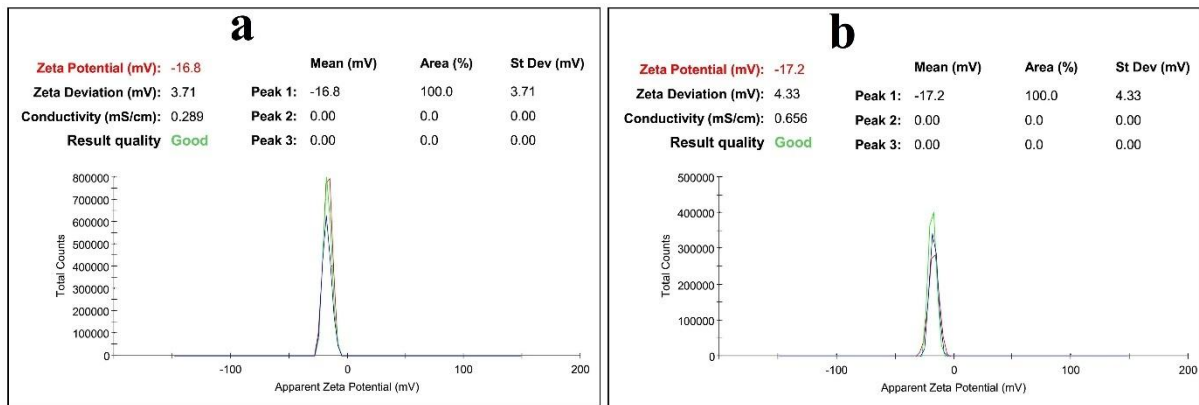


Figure 5. Zeta potential for (a) HPAC@MNPs (b) HPAC@MNPS-MRN

pH-dependent release behavior

Figure 6 displays the total amount of MRN released in HPAC@MNPs at pH 5.4 and pH 7.4, both at a temperature of 37 °C. After analyzing different pH values for MRN release, it was noted that the release of MRN varied depending on the pH level. Specifically, MRN exhibited a higher level of release in natural or normal conditions (Cunha et al., 2023). In order to conduct the release studies, solutions containing 10 mL of MRN loaded into HPAC@MNPs at concentrations of 93 µg/mL were utilized. These solutions were prepared at various pH levels and concentrations.

At pH 7.4, the MRN release from HPAC@MNPs was 31.88% after 24 hours, however at pH 5.4, this rate was 16.22%. When loaded MRN was released in HPAC@MNPs at a pH of 5.4, the release was 11.92% after six hours, 14.26% after twelve hours, and 16.28% after forty-eight hours. When loaded MRN was released in HPAC@MNPs at a pH of 7.4, the release was 23.57% after six hours, 27.81% after twelve hours, and 31.52% after forty-eight hours.

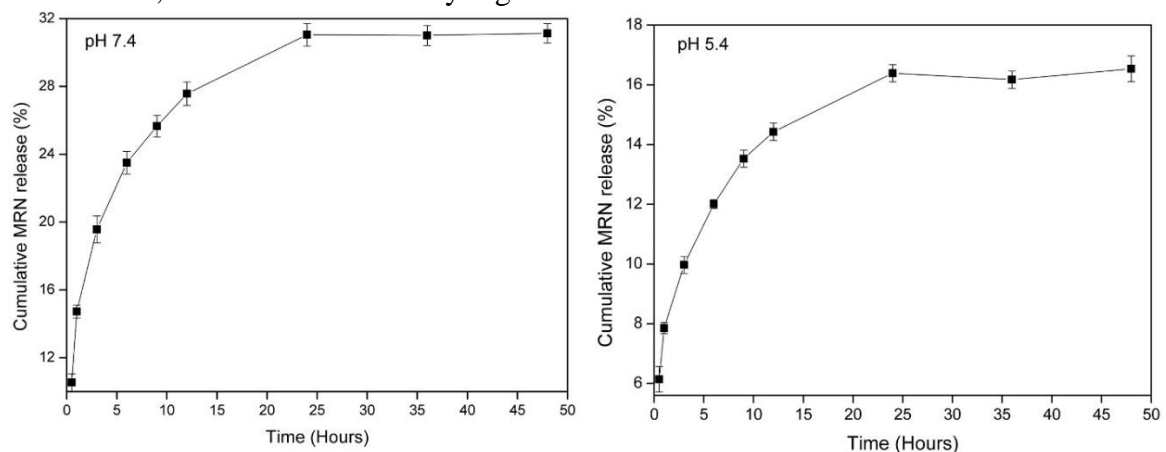


Figure 6. Release of MRN loaded in HPAC@MNPs at pH 5.4 and pH 7.4

Cytotoxic Studies

In this study, MCF-7 breast cancer, U373 glioblastoma model were used as cell lines (Józwiak et al., 2020; Palei et al., 2023). Furthermore, HUVEC was utilized as a healthy cell line throughout the course of this research (Meng et al., 2021). The MTT assay was used to examine the cytotoxic effects of MRN loaded in HPAC@MNPs on MCF-7, U373, and HUVEC cell lines. Among the colorimetric assays that are utilized the most frequently is the MTT test, which involves the reduction of a tetrazolium compound (MTT) to formazan. The use of colorimetric tests is widespread because they are applied for the goal of measuring cellular metabolic activity, which is a sign of toxicity (Choi et al., 2022).

The effects of pH 7.4 and 5.4 solutions prepared in phosphate buffer on cell viability of MCF-7, U373 and HUVEC cell lines and MRN release of HPAC@MNPs-MRN were evaluated after 24 and 48 hours. After 24 hours of exposure with MRN-loaded HPAC@MNPs at pH 7.4 (Figure 7), a 13% and 5% decrease was observed for 200 $\mu\text{g}/\text{mL}$ in the tested MCF-7 and U373 cell lines, respectively, while no visible decrease in cell viability was observed at other concentrations. After 48 hours of exposure with MRN-loaded HPAC@MNPs at pH 7.4 (Figure 7), a 6% and 7% decrease was observed for 200 $\mu\text{g}/\text{mL}$ in the tested MCF-7 and U373 cell lines, respectively, while no visible change in cell viability was observed at other concentrations.

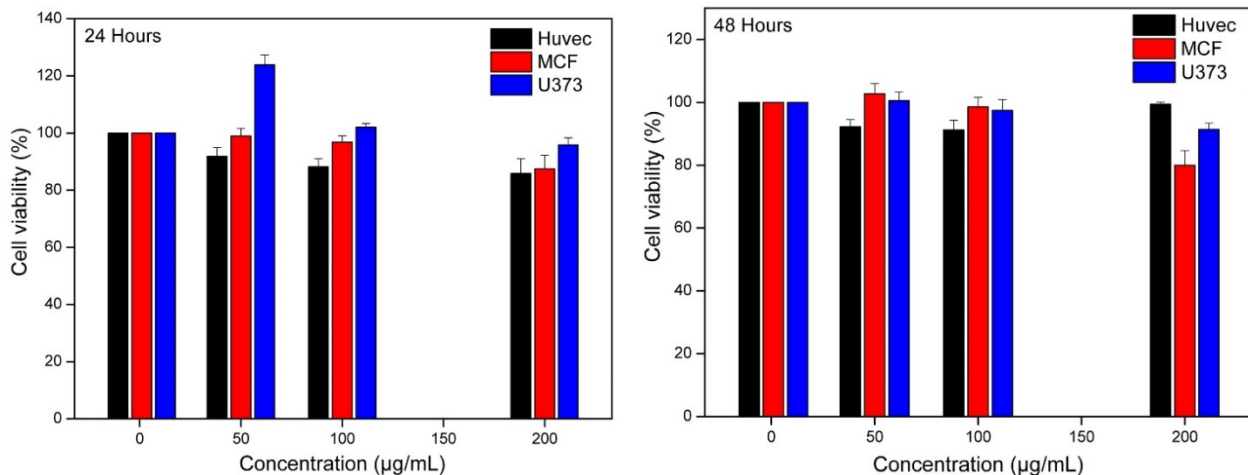


Figure 7. Effect of HPAC@MNPs-MRN (1–200 $\mu\text{g}/\text{mL}$ prepared with PBS 7.4 buffer) on cell viability of HUVEC, MCF-7 and U373 cell lines

24 h exposure with MRN-loaded HPAC@MNPs at pH 5.4 (Figure 8) showed 8%, 11%, and 12% decrease in cell viability for 50, 100, and 200 $\mu\text{g}/\text{mL}$ in the tested MCF-7 cell line, respectively, while an 8.5% decrease in cell viability was observed only for 200 $\mu\text{g}/\text{mL}$ in the U373 cell line. 48 h exposure with MRN-loaded HPAC@MNPs at pH 5.4 (Figure 8) showed 16%, 21%, and 21% decrease in cell viability for 50, 100, and 200 $\mu\text{g}/\text{mL}$ in the tested MCF-7 cell line, respectively, while an 8%, 9%, and 9% decrease in cell viability was observed in the U373 cell line, respectively, while an 8%, 9%, and 9% decrease in cell viability was observed for 50, 100, and 200 $\mu\text{g}/\text{mL}$ in the tested MCF-7 cell line,

respectively.

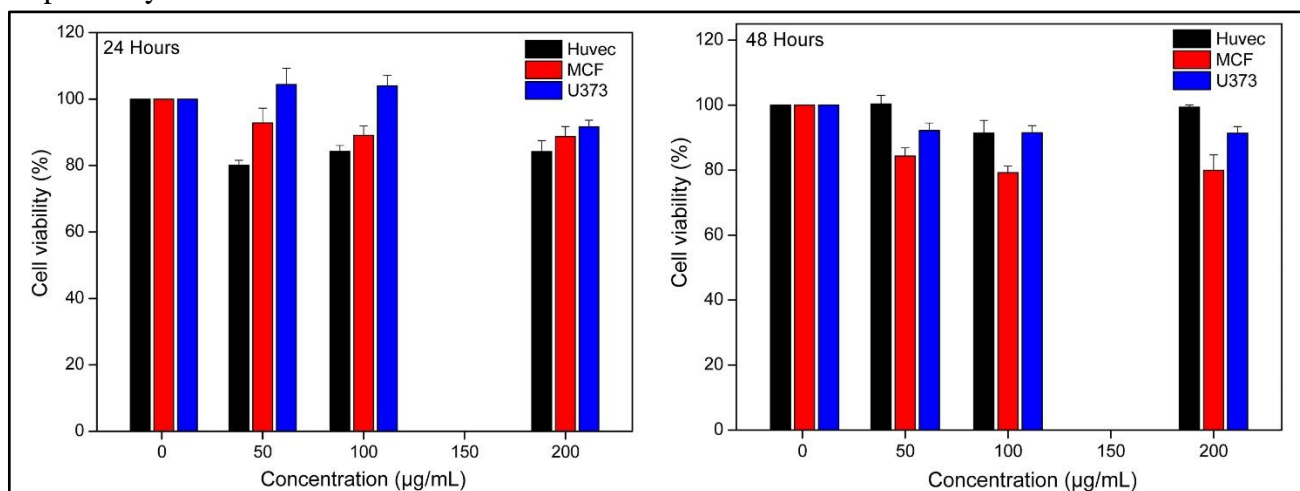


Figure 8. Effect of HPAC@MNPs-MRN (1–200 µg/mL prepared with PBS 5.4 buffer) on cell viability of HUVEC, MCF-7 and U373 cell lines

CONCLUSION

In this research, HPAC@MNPs were synthesized to transport MRN, one of the drugs used in the treatment of cancer, to the target area. The HPAC@MNPs and HPAC@MNPs-MRN nanocomposite were characterized using the techniques of FTIR, SEM, DLS, and Zeta potential. The MRN was effectively introduced into HPAC@MNPs by a 24-hour incubation method. In this study, when pH 5.4 was compared with pH 7.4, it was found that MRN release was greater at pH 5.4. This can be attributed to the higher encapsulation efficiency of MRN resulting from the increased solubility and dissolution rate of the MRN drug due to the acidic nature of the tumor site. This improvement is a result of the drug transforming into a different form after being loaded into HPAC@MNPs. This indicates that MRN-loaded HPAC@MNPs have the potential to be an effective nanodelivery technology for the treatment of MCF-7 and U373. The cytotoxic effects of HPAC@MNPs-MRN on cell viability were observed in U373 (glioblastoma) and MCF-7 (breast), and these effects were observed in a way that was both concentration and time dependent. Particularly the MCF-7 cell lines exhibited greater sensitivity in terms of cell viability when compared to U373. While additional biological investigations conducted in laboratory settings and living organisms are necessary, our results suggests that HPAC@MNPs-MRN have potential as targeted treatment systems for diseases caused by damage. This is particularly evident in their impact on MCF-7 cell lines.

Conflict of Interest

The article authors declare that there is no conflict of interest between them.

Author's Contributions

The authors declare that they have contributed equally to the article.

REFERENCES

- Aisida, S.O., Akpa, P.A., Ahmad, I., Zhao, T.K., Maaza, M., & Ezema, F.I. (2020). Bio-inspired encapsulation and functionalization of iron oxide nanoparticles for biomedical applications. *European polymer journal*, 122, 109371.
- Attia, M., Glickman, R.D., Romero, G., Chen, B., Brenner, A.J., & Ye, J.Y. (2022). Optimized metal-organic-framework based magnetic nanocomposites for efficient drug delivery and controlled release. *Journal of Drug Delivery Science and Technology*, 76, 103770.
- Baig, M.M.F.A., Fatima, A., Gao, X., Farid, A., Khan, M.A., Zia, A.W., & Wu, H. (2022). Disrupting biofilm and eradicating bacteria by Ag-Fe₃O₄@ MoS₂ MNPs nanocomposite carrying enzyme and antibiotics. *Journal of Controlled Release*, 352, 98-120.

- Baran, A., Ertaş, E., Baran, M.F., Eftekhari, A., Gunes, Z., Keskin, C., Khalilov, R. (2024). Green-Synthesized Characterization, Antioxidant and Antibacterial Applications of CtAC/MNPs-Ag Nanocomposites. *Pharmaceuticals*, 17(6), 772.
- Baran, M. F., Keskin, C., Baran, A., Kurt, K., İpek, P., Eftekhari, A., & Cho, W.C. (2023). Green synthesis and characterization of selenium nanoparticles (Se NPs) from the skin (testa) of *Pistacia vera* L. (Siirt pistachio) and investigation of antimicrobial and anticancer potentials. *Biomass Conversion and Biorefinery*, 1-11.
- Barrios, C.H. (2022). Global challenges in breast cancer detection and treatment. *The Breast*, 62, S3-S6.
- Choi, B.H., Kim, M.R., Jung, Y.N., Kang, S., & Hong, J. (2022). Interfering with color response by porphyrin-related compounds in the MTT tetrazolium-based colorimetric assay. *International Journal of Molecular Sciences*, 24(1), 562.
- Cunha, C., Marinheiro, D., Ferreira, B.J., Oliveira, H., & Daniel-da-Silva, A.L. (2023). Morin hydrate encapsulation and release from mesoporous silica nanoparticles for melanoma therapy. *Molecules*, 28(12), 4776.
- De Gaetano, F., Margani, F., Barbera, V., D'Angelo, V., Germanò, M.P., Pistarà, V., & Ventura, C.A. (2023). Characterization and In Vivo Antiangiogenic Activity Evaluation of Morin-Based Cyclodextrin Inclusion Complexes. *Pharmaceutics*, 15(9), 2209.
- Józwiak, M., Filipowska, A., Fiorino, F., & Struga, M. (2020). Anticancer activities of fatty acids and their heterocyclic derivatives. *European journal of pharmacology*, 871, 172937.
- Kamrani, A., Hosseinzadeh, R., Shomali, N., Heris, J.A., Shahabi, P., Mohammadinasab, R., Akbari, M. (2023). New immunotherapeutic approaches for cancer treatment. *Pathology-Research and Practice*, 248, 154632.
- Karimian, A., Mohammadrezaei, F.M., Moghadam, A.H., Bahadori, M.H., Ghorbani-Anarkooli, M., Asadi, A., & Abdolmaleki, A. (2022). Effect of astaxanthin and melatonin on cell viability and DNA damage in human breast cancer cell lines. *Acta Histochemica*, 124(1), 151832.
- Kovrigina, E., Chubarov, A., & Dmitrienko, E. (2022). High drug capacity doxorubicin-loaded iron oxide nanocomposites for cancer therapy. *Magnetochemistry*, 8(5), 54.
- Meng, Q., Pu, L., Lu, Q., Wang, B., Li, S., Liu, B., & Li, F. (2021). Morin hydrate inhibits atherosclerosis and LPS-induced endothelial cells inflammatory responses by modulating the NFκB signaling-mediated autophagy. *International Immunopharmacology*, 100, 108096.
- Palei, N.N., Mounika, G., Mohanta, B.C., & Rajangam, J. (2023). Quercetin and Morin dual drug loaded nanostructured lipid carriers: formulation and in vitro cytotoxicity study on MCF7 breast cancer cells. *Journal of Dispersion Science and Technology*, 1-9.
- Peng, L., Qin, P., Lei, M., Zeng, Q., Song, H., Yang, J., Gu, J. (2012) Modifying Fe₃O₄ nanoparticles with humic acid for removal of Rhodamine B in water. *Journal of Hazardous Materials*, 209, 193-198.
- Saif, B., Wang, C., Chuan, D., & Shuang, S. (2015). Synthesis and characterization of Fe₃O₄ coated on APTES as carriers for morin-anticancer drug. *Journal of Biomaterials and Nanobiotechnology*, 6(4), 267-275.
- Santhosh, A., & Dawn, S.S. (2021). Synthesis of zinc chloride activated eco-friendly nano-adsorbent (activated carbon) from food waste for removal of pollutant from biodiesel wash water. *Water Science and Technology*, 84(5), 1170-1181.
- Setia, A., Mehata, A.K., Malik, A.K., Viswanadh, M.K., & Muthu, M.S. (2023). Theranostic magnetic nanoparticles: synthesis, properties, toxicity, and emerging trends for biomedical applications. *Journal of Drug Delivery Science and Technology*, 81, 104295.
- Shabatina, T.I., Vernaya, O.I., Shabatin, V.P., & Melnikov, M.Y. (2020). Magnetic nanoparticles for biomedical purposes: Modern trends and prospects. *Magnetochemistry*, 6(3), 30.
- Sleeman, K.E., Gomes, B., de Brito, M., Shamieh, O., & Harding, R. (2021). The burden of serious health-related suffering among cancer decedents: Global projections study to 2060. *Palliative medicine*, 35(1), 231-235.
- Taguchi, K., Tano, I., Kaneko, N., Matsumoto, T., & Kobayashi, T. (2020). Plant polyphenols Morin and Quercetin rescue nitric oxide production in diabetic mouse aorta through distinct pathways. *Biomedicine & Pharmacotherapy*, 129, 110463.
- Trendafilova, I., Mihály, J., Momekova, D., Chimshirova, R., Lazarova, H., Momekov, G., & Popova, M. (2020). Antioxidant activity and modified release profiles of Morin and hesperetin flavonoids loaded in Mg-or Ag-modified SBA-16 carriers. *Materials Today Communications*, 24, 101198.
- Tural, B., Ertaş, E., Batıbay, H., & Tural, S. (2024). Comparative Study on Silver Nanoparticle Synthesis Using Male and Female *Pistacia Khinjuk* Leaf Extracts: Enhanced Efficacy of Female Leaf Extracts. *ChemistrySelect*, 9(30), e202402117.
- Venskutonis, P.R. (2018). Phytochemical composition and bioactivities of hawthorn (*Crataegus* spp.): Review of recent research advances. *Journal of Food Bioactives*, 4, 69-87.